Биохимия

Biochemistry

УДК 577.32571.27

In silico АНАЛИЗ ДИМЕРИЗАЦИИ PD-L1, ИНДУЦИРОВАННОЙ РЕСВЕРАТРОЛОМ[1]

***В. А. УРБАН*[1)], *А. И. ДАВИДОВСКИЙ*[1)], *В. Г. ВЕРЕСОВ*[1)]**

[1)]*Институт биофизики и клеточной инженерии НАН Беларуси, ул. Академическая, 27, 220072, г. Минск, Беларусь*

Активация Т-клеток через блокаду взаимодействий PD-1 и PD-L1 рассматривается как одна из наиболее перспективных стратегий в лечении рака. Ряд антител, таргетирующих сигнальный путь иммунного чек-пойнта PD-1 и PD-L1, были одобрены для применения после успешных клинических испытаний. Однако использование антител сопряжено с такими недостатками, как низкая проницаемость в ткани и опухоли, плохие биодеградация и оральная биодоступность, высокая стоимость производства. Применение низкомолекулярных соединений может позволить устранить недостатки, имеющие место при использовании антител, ингибирующих иммунные чек-пойнты. В настоящее время более 20 низкомолекулярных ингибиторов взаимодействия PD-1 и PD-L1, базовая структура которых основывается на замещенных группах бифенила, связанного с ароматическим кольцом посредством бензилэфирной связи, были идентифицированы и запатентованы компанией *Бристол – Майерс – Сквибб* (США). Структурные исследования показали, что все эти соединения действуют посредством индукции димеризации PD-L1, делая белок PD-L1 некомпетентным для взаимодействия с PD-1. Недавно выявлено, что ресвератрол ингибирует взаимодействие PD-1 и PD-L1, также индуцируя димеризацию PD-L1, однако механизмы

[1]Материал статьи представлен в виде доклада на Международной научной конференции «Молекулярные, мембранные и клеточные основы функционирования биосистем», проводившейся в рамках XIV съезда Белорусского общественного объединения фотобиологов и биофизиков (Минск, 17–19 июня 2020 г.).

Образец цитирования:
Урбан ВА, Давидовский АИ, Вересов ВГ. *In silico* анализ димеризации PD-L1, индуцированной ресвератролом. *Журнал Белорусского государственного университета. Биология.* 2021;1:39–47 (на англ.).
https://doi.org/10.33581/2521-1722-2021-1-39-47

For citation:
Urban VA, Davidovskii AI, Veresov VG. *In silico* analysis of resveratrol induced PD-L1 dimerisation. *Journal of the Belarusian State University. Biology.* 2021;1:39–47.
https://doi.org/10.33581/2521-1722-2021-1-39-47

Авторы:
Виктор Андреевич Урбан – младший научный сотрудник лаборатории иммунологии и клеточной биофизики.
Александр Игоревич Давидовский – младший научный сотрудник лаборатории иммунологии и клеточной биофизики.
Валерий Гавриилович Вересов – доктор биологических наук; главный научный сотрудник лаборатории иммунологии и клеточной биофизики.

Authors:
Viktor A. Urban, junior researcher at the laboratory of immunology and cell biophysics.
urban@ibp.org.by
Alexander I. Davidovskii, junior researcher at the laboratory of immunology and cell biophysics.
davidovskii@ibp.org.by
Valery G. Veresov, doctor of science (biology); chief researcher at the laboratory of immunology and cell biophysics.
veresov@ibp.org.by

этого остаются неясными. В настоящей работе использованы инструменты вычислительной структурной биологии (построение моделей белок – белок и белок – лиганд в сочетании с методом молекулярной динамики) в целях установления структурных механизмов димеризации PD-L1, индуцированной ресвератролом.

Ключевые слова: PD-1; PD-L1; ресвератрол; вычислительная структурная биология.

Благодарность. Настоящая работа выполнена в рамках государственной программы научных исследований «Биотехнологии» (грант № 1.45).

In silico ANALYSIS OF RESVERATROL INDUCED PD-L1 DIMERISATION

***V. A. URBAN*[a], *A. I. DAVIDOVSKII*[a], *V. G. VERESOV*[a]**

[a]*Institute of Biophysics and Cell Engineering, National Academy of Sciences of Belarus, 27 Akademičnaja Street, Minsk 220072, Belarus*

Corresponding author: V. G. Veresov (veresov@ibp.org.by)

T-cell activation through the blockade of PD-1 – PD-L1 interactions is recognised at present as one of the most promising strategies in the cancer treatment and a number of antibodies targeting the PD-1 – PD-L1 immune checkpoint pathway have been approved after successful clinical trials. However, the use of antibodies suffers from a number of shortcomings including poor tissue and tumor penetration, long half-life time, poor oral bioavailability, and expensive production costs. Small molecule based therapeutic approaches offer the potential to address the shortcomings of the antibody-based checkpoint inhibitors. At present, more than twenty small molecular inhibitors of the PD-1 – PD-L1 interactions whose scaffold is based on substituted biphenyl group connected to a further aromatic ring through a benzyl ether bond have been identified and patented by *Bristol – Mayers – Squibb* (USA). Structural studies have shown that all these compounds act by inducing the dimerisation of PD-L1 that makes PD-L1 non-competent for forming complex with PD-1. Very recently, the dietary polyphenol resveratrol (RSV) has been reported to inhibit the PD-1 – PD-L1 interactions through the induction of the PD-L1 dimerisation but the mechanisms remain unclear. Here, computational structural biology tools combining protein – protein and protein – ligand docking with molecular dynamics simulations were used to gain structural insights into the mechanisms of the RSV-induced dimerisation of PD-L1.

Keywords: PD-1; PD-L1; resveratrol; computational structural biology.

Acknowledgements. This work was supported by the Belarusian state program for biotechnology (grant No. 1.45).

Introduction

Among different therapeutic options, cancer immunotherapy has emerged most recently as a powerful strategy for treating various types of cancers [1–3]. Tumor cells express cancer-specific antigens derived from genetic alterations, and as such have to be targeted by the immune cells. However, cancer cells have adapted to escape this host defense mechanism by exploiting endogenous T-cell immune tolerance pathways, termed immune checkpoints [4; 5]. The major among them is the PD-1 (programmed death 1) and PD-L1 (programmed death ligand 1) immune checkpoint signaling pathway. PD-1 protein suppresses T-cell cytolytic function when bound to its ligand PD-L1 [4; 5]. PD-L1 is upregulated on antigen-presenting cells in most cancer types via induction of PD-L1 expression by γIFN (secreted from tumor infiltrating T-cells) and by constitutive expression of PD-L1 resulting from oncogene activation [4–6]. Indeed, the presence of PD-L1 in the tumor microenvironment is generally correlated with poor prognosis in multiple cancer types [7]. Therefore, one may expect that antagonising the protein – protein interactions of PD-1 with its ligands (PD-L1 and PD-L2) can revert T-cell phenotypic exhaustion and thus result in the efficient killing of cancer cells. In line with this, antibodies that target PD-1 or its binding to PD-L1 have shown unprecedented rates of durable clinical responses in patients with various cancer types [4]. These antibodies have been successful as single agents in numerous clinical trials and have revolutionised the field of antitumor immunoterapy. However, due to lower production costs, higher stability, improved tumour penetration, amenability for oral administration and elimination of immunogenicity, small-molecular weight inhibitors present a more promising option as compared to antibodies as immune check point inhibitors. Despite these potential advantages of small molecule inhibitors (SMIs), their discovery has greatly lagged behind mABs. This is likely because PD-1 and PD-L1 proteins are predicted to be challenging drug targets for small molecules [8] since the PD-1 – PD-L1 interaction interface is large (1970 $Å^2$) and lacks deep hydrophobic pockets traditionally found in more druggable proteins [9]. In spite of

this, to date, more than twenty small molecule antagonists that directly and selectively disrupt the association between PD-1 and PD-L1 have been identified and disclosed in several patents authored by *Bristol – Mayers – Squibb* (BMS) [10]. The affinities of these compounds towards PD-L1 determined with the use of the homogenous time-resolved fluorescence assay and application of the europium cryptate-labeled anti-Ig were in the range of 0.6 nmol/L up to 20 μmol/L for IC_{50} values. Recently, the dietary polyphenol resveratrol, a natural polyphenolic phytoalexin that is present in red wine, red grape skin, berries, peanuts, and other natural sources, has been shown to enhance anti-tumor T-cell immunity, supposedly also by the stabilisation of inactive trimeric structure, including two PD-L1 molecules and small molecular ligand, thus using indirect way of the PD-1 – PD-L1 axis inhibition [11], however the structural insights into this process is absent. Here, computational structural biology tools combining protein – protein and protein – ligand docking with molecular dynamics simulations were used to gain structural insights into the mechanisms of the resveratrol induced dimerisation of PD-L1 as well as the elucidation of structural determinants of its high inhibiting activity.

Materials and methods

Predicting the 3D structures of the PD-L1 – resveratrol complex. First, the coarse-grained model of the PD-L1 dimer – resveratrol structure complex was predicted using the *Glide* program of the protein – ligand docking [12]. In doing so, the protein was considered as rigid, whereas the ligand was treated as flexible. Because the known experimental PD-L1 dimer structures when complexed with different BMS-ligands (PDB codes: 5j8o, 5j89, 5n2d, 5n2f, 5niu, 5nix, 6nm7, 6nm8) differ from one another, all these dimers were preliminary analysed using *Glide* in terms of their interaction with resveratrol, and the lowest-energy configuration including the protein dimer and ligand was selected to be used in subsequent molecular dynamics (MD) simulations. Because BMS-ligands are known to bind to PD-L1 in extracellular environment [12], whereas the membrane parts of PD-L1 monomers are positioned far apart and therefore do not interact, the similar situation was proposed for PD-L1 interaction with resveratrol. Taking this into account and for the sake of simplicity, membrane parts of PD-L1 were omitted from MD simulations. MD simulations were performed using the *GROMACS* software [14] with the CHARMM36 all-atom force field [15]. The protein was solvated using the TIP3P water model [16] in a dodecahedron box of 44 × 37 × 34 Å and counterions were added to keep systems neutral. Periodic boundary conditions were applied and Lennard-Jones interactions were truncated at 12 Å with a force switch smoothing function from 10 to 12 Å. The integration time step was 2.0 fs. The non-bonded interaction lists were generated with a cutoff distance of 16 Å. The V-rescale thermostat [17] was used to maintain the temperature at 300 K and the Parrinello – Rahman barostat for maintaining the pressure at 1 bar [18]. Electrostatic interactions were calculated explicitly at a distance smaller than 1.0 nm, long-range electrostatic interactions were treated by particle mesh Ewald summation at every step [19]. After 500 steps steepest descent minimisation with the protein fixed and another 200 steps without the protein fixed, the systems were first heated to 300 K and then subjected to a 100 ps canonical ensemble (NVT) simulation followed by a 100 ps isothermal – isobaric ensemble (NPT) simulation. After a subsequent 1 ns NPT simulation as equilibration, the production simulations were run for 300 ns in the NVT ensemble with the Verlet leap-frog algorithm coupled with mesh Ewald method for long-range electrostatics and Verlet cut-off with the distance of 1 nm for short-range interactions [20]. GPU-acceleration was used in all MD simulations. The estimation of the binding affinity of resveratrol to PD-L1 or the PD-L1 dimer was carried out using three different metrics: *Glide* score [12], Prodigy-Lig affinity [21] and Kdeep affinity [22]. General characterisation of protein – ligand interactions was carried out using protein – ligand interaction profiler (PLIP) [23].

Modeling PD-L1 – PD-L1 interaction within the PD-L1 dimer – resveratrol complex. The modeling of PD-L1 **–** PD-L1 interaction was performed in **a** stepwise fashion using **a** four-staged computational molecular docking protocol ((PIPER [24] + GRAMM-X [25] + HDock [26]) – RosettaDock [27; 28] – GalaxyRefineComplex [29] – RosettaDock (abbreviated by $(P + G + H)R_DG_{RC}R_D$)), where PIPER performs exhaustive global rigid-body search of rigid-body docking decoys, GRAMM-X and HDOCK combine free rigid-body search with the template-based one. Next the top-ranked decoys were first refined by the GalaxyRefineComplex approach during the second stage, followed by the refinement using the RosettaDock approach in the third stage. When employing GalaxyRefineComplex in the second stage of the full protocol of the decoy set generation, the refinement procedure was applied to a set of several top-scored protein complexes that had been obtained at the first stage using the P + G + H combination. To discriminate the near-native complexes among the decoys, the binding affinities together with the RosettaDock energy funnels and the total energy score decrease upon binding were used in consensus manner. We estimated the binding affinities by two different ways: as interface score of RosettaDock [27; 28] and as ΔG provided by the Prodigy server [30]. In addition, we estimated buried surface area (BSA), geometric complementarity (interface van der Waals energy), number of salt bridges and hydrogen bonds as main determinants of binding affinity [31; 32]. The Rosetta3 [33] interface analyser was

used to evaluate BSA, whereas the PPCheck server [34] was used to estimate van der Waals energy, number of salt bridges and hydrogen bonds. All these metrics, which are based on essentially different physical concepts, were used in consensus manner to strengthen the reliability of functional conclusions based on affinity estimates. Since the availability of a low-energy template-based hit upon template-based docking can be viewed as an equivalent of the knowledge of the binding site location, we considered the similarity between the relative positions of proteins-partners in the final model and those in the highest-ranked rigid-body decoy obtained by the template-based docking as an additional and important indication of the successful prediction.

Results and discussion

The evaluation of the affinities between resveratrol and PD-L1 dimers from atomistic complexes of BMS-ligands with PD-L1. To establish the structure of the PD-L1 – resveratrol protein – ligand complex, the structures of the aPD-L1 and bPD-L1 dimers from 5j8o, 5niu, 5nix, 5j89, 6nm7, 6nm8 were subjected to liganding by resveratrol using the *Glide* program of the protein – ligand docking [12]. In doing so, the protein was considered as rigid, whereas the ligand was treated as flexible. Next, the affinities of the PD-L1 dimers – resveratrol complexes were estimated using two different metrics: *Glide* score [12], and Prodigy-Lig affinity [21]. The consensus lowest-energy structure was saved to be used in subsequent MD refinements. The results of this preliminary analysis is shown in table 1.

Table 1

Free energy estimates of the interactions between PD-L1 dimers from 5j8o, 5niu, 5j89, 5n2d, 5n2f, 6nm7, 6nm8, 6r3k atomistic structures and resveratrol, kcal/mol

PDB code of the PD-L1 dimer structure used	ΔG_{Glide}	ΔG_{Pr}	ΔG_{AB}	$\Delta G_{Pr,trimer}$
5j8o(1)	–7.95	–13.7	–7.3	–21.0
5j8o(2)	–7.90	–13.8	–7.3	–21.1
5niu(1)	–8.19	–14.0	–7.5	–21.5
5niu(2)	–7.56	–13.9	–7.5	–21.4
5niu(3)	–7.33	–13.9	–7.5	–21.4
5n2d(1)	–7.59	–13.8	–7.1	–20.9
5n2d(2)	–7.55	–13.8	–7.1	–20.9
5n2d(3)	–7.53	–13.8	–7.1	–20.9
5n2f(1)	–8.54	–13.7	–7.6	–21.3
5n2f(2)	–8.46	–13.8	–7.6	–21.4
5n2f(3)	–8.45	–13.7	–7.6	–21.3
6r3k(1)	–7.21	–13.7	–6.4	–20.6
6r3k(2)	–7.15	–13.7	–6.4	–20.6
6r3k(3)	–7.09	–13.7	–6.4	–20.6
5j89(1)	–7.48	–13.9	–7.9	–21.8
5j89(2)	–7.45	–13.9	–7.9	–21.8
5j89(3)	–7.35	–13.9	–7.9	–21.8
5j89(4)	–7.32	–13.8	–7.9	–21.7
6nm7(1)	–8.98	–14.1	–8.0	–22.1
6nm7(2)	–8.81	–14.1	–8.0	–22.1
6nm8(1)	–8.06	–13.8	–7.7	–21.5
6nm8(1)	–8.00	–13.8	–7.7	–21.5

Note. ΔG_{Glide}, ΔG_{Pr} are binding affinities obtained using *Glide* and Prodigy respectively; ΔG_{AB} is the interprotein binding affinities between PD-L1 monomers A and B; $\Delta G_{Pr,trimer} = \Delta G_{Pr} + \Delta G_{AB}$.

From the results that have been obtained the complex of resveratrol with the PD-L1 dimer that was adopted from 6nm7(1) structure was saved to be used in further refinement.

The refinement of the PD-L1 dimer – resveratrol complex using MD simulations. The best-scored PD-L1 dimer – resveratrol structure obtained by *Glide* (with PD-L1 dimer structure adopted from 6nm7) was next subjected to MD simulations as described in the section «Materials and methods». The root mean square deviation (RMSD) and the root mean square fluctuation (RMSF) were employed to characterise the motions of the ligand in respect to the protein and the stabilisation of the trimeric complex. The plots depicting RMSD and RMSF are shown in fig. 1 and 2 respectively.

The plot depicts structural stability, positioning and motion of resveratrol upon the formation of the complex with the PD-L1 dimer.

Our findings show that the systems converged and attained stability early in the production run after 50 ns for the PD-L1 dimer – resveratrol complex. The final structure of the MD simulations was considered as the structure of the complex (fig. 3). A comparison between the predicted structure and that obtained by docking with *Glide* has shown a significant change both in the conformation and orientation of PD-L1 molecules in all cases with RMSD of 1.122 Å. The analysis of the PD-L1 dimer – resveratrol complex structure using the PLIP [23] revealed the formation of 16 hydrophobic contacts and five hydrogen bonds (see fig. 3, table 2).

The analysis of the protein – ligand binding affinity by Prodigy-Lig [21] resulted in binding affinity values between the PD-L1 dimer and resveratrol of –14.2. The most important results of simulations are given in table 3. The modeling has shown a rather high intermolecular shape and polar complementarity in the PD-L1 – PD-L1 – resveratrol complex thus explaining the induction of PD-L1 dimerisation and inhibition of PD-1 – PD-L1 interaction. Of note, ΔG_{Glide} for interaction with resveratrol is higher than that for interaction with BMS-ligands, whereas with ΔG_{Pr} the lowest value takes places namely with resveratrol. Nearly the same value (–9.252 kcal/mol) has been earlier obtained with *AutoDock* [35]. This discrepancy can be explained by more accurate account of van der Waals interactions by Prodigy as compared with *Glide* or *AutoDock* [35].

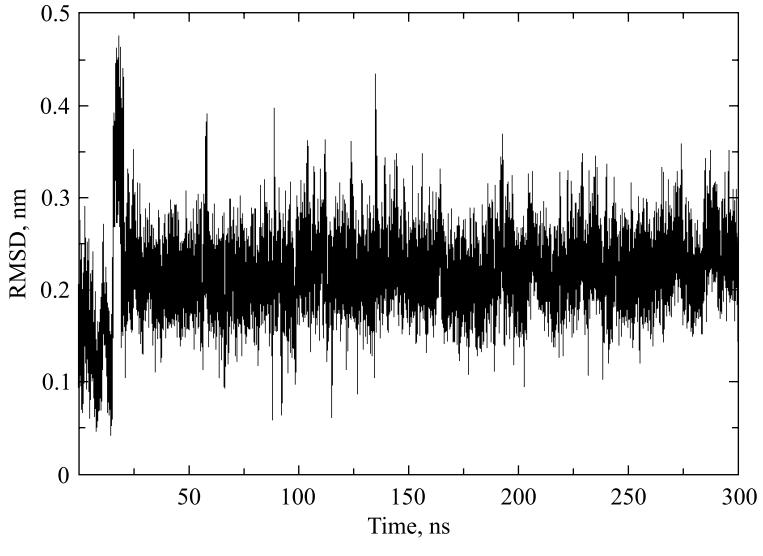

Fig. 1. Resveratrol atoms RMSD during MD simulations

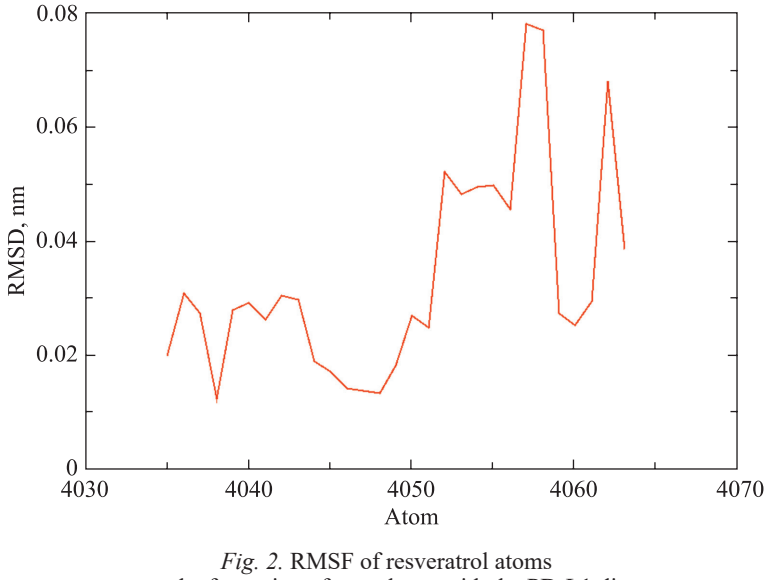

Fig. 2. RMSF of resveratrol atoms
upon the formation of complexes with the PD-L1 dimer

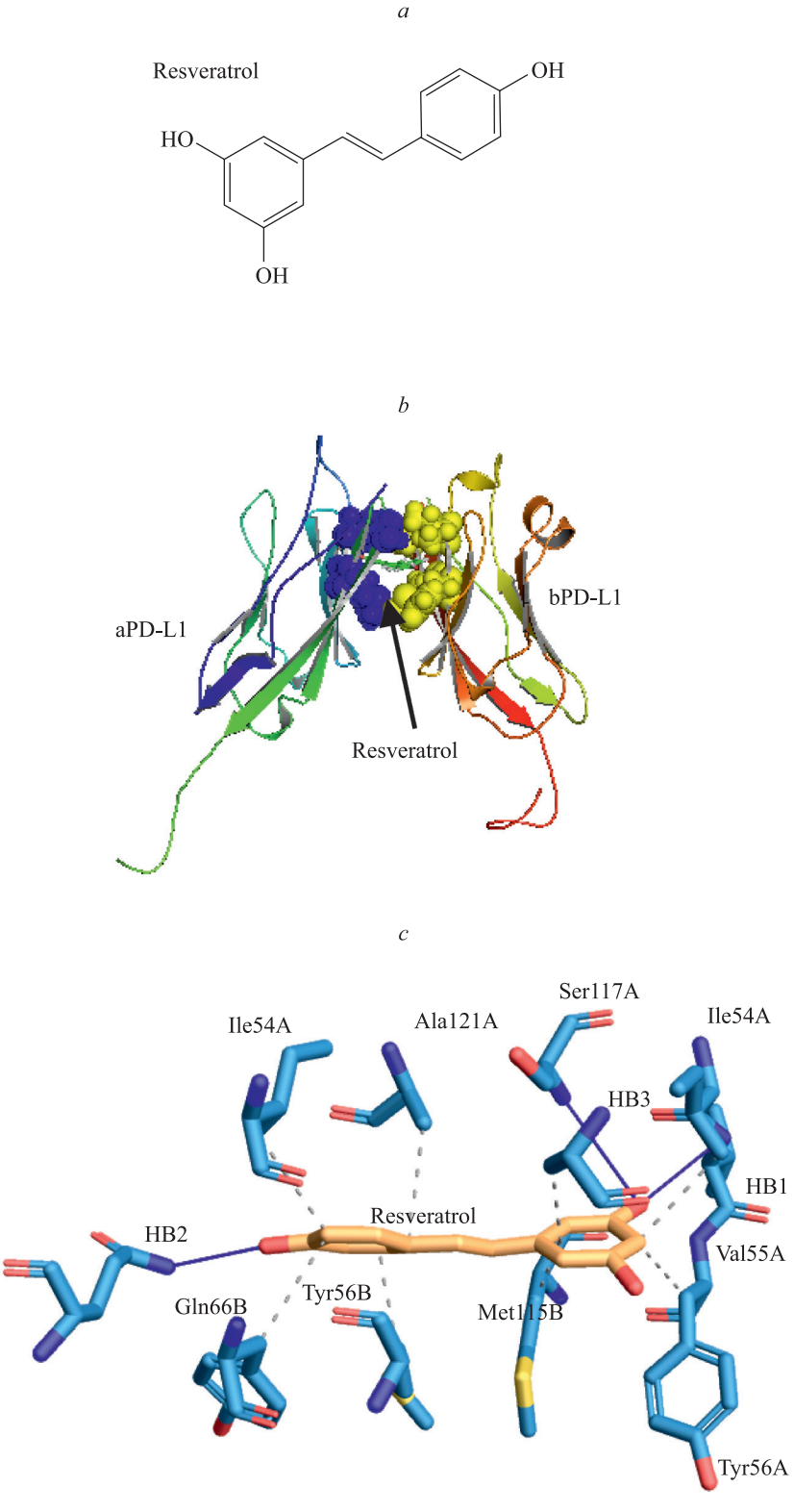

Fig. 3. Structure of the PD-L1 dimer – resveratrol complex: *a* – chemical structure of resveratrol; *b* – predicted 3D structure of the extracellular part of PD-L1 dimer in complex with resveratrol after 300 ns MD simulations (resveratrol arrangement between two PD-L1 immunoglobulin domains is shown); *c* – the closer view of the PD-L1 dimer – resveratrol interface. Hydrogen bonds (HB1, HB2 and HB3) are shown as blue lines. The hydrophobic contacts are shown as dotted black lines

Table 2

Hydrophobic and polar contacts between resveratrol and PD-L1 dimer

Index	Residue	AA(atom)	Distance, Å	Ligand atom
Hydrophobic contacts				
1_HPH*	54A	Ile(CD2)	3.55	C11
2_HPH*	54B	Ile(CG2)	3.32	H21
3_HPH	56A	Tyr(CG)	3.33	C13
4_HPH	56B	Tyr(CD1)	2.72	C11
5_HPH	56B	Tyr(CG)	3.28	C6
6_HPH	66A	Gln(HG2)	2.89	H25
7_HPH	115A	Met(CB)	3.59	C9
8_HPH	115B	Met(CB)	3.79	C6
9_HPH	116B	Ile(HG12)	3.71	H25
10_HPH	117A	Ser(HB2)	3.74	H20
11_HPH	117B	Ser(CB)	3.70	H28
12_HPH	121A	Ala(CB)	3.54	C3
13_HPH	121B	Ala(CB)	3.40	C11
14_HPH	122A	Asp(N)	3.52	H24
15_HPH	123B	Tyr(CB)	3.31	H26
16_HPH	122B	Asp(HB2)	3.52	H27
Hydrogen bonds				
1_HB**	56B	Tyr(OH)	3.61	O16
2_HB	66B	Gln(N)	3.43	O7
3_HB	117A	Ser(N)	3.57	O16
4_HB	122B	Asp(H)	3.97	O7
5_HB	123B	Tyr(HB2)	2.32	O16

*HPH stands for hydrophobic contacts. **HB stands for hydrogen bonds.

Table 3

The most important results of interactions between resveratrol, BMS-8, BMS-37, BMS-200, BMS-202, BMS-1001, BMS-1166, BMS-105 and PD-L1 dimer

Protein – ligand complexes	IC_{50}, nmol/L	ΔG_{Pr}, kcal/mol	ΔG_{Glide}, kcal/mol	ΔG_{AB}, kcal/mol	$\Delta G_{Pr,tr}$** kcal/mol	n_{HPH}	n_{HB}	n_{SB}	$n_{\pi\text{-st}}$	PD-L1 dimer RMSD from $(PD\text{-}L1)_2$, in complex with BMS-8
PD-L1 dimer – resveratrol	1–10	–14.1	–9.0	–8.0	–22.2	15	5	0	0	1.12
PD-L1 dimer – BMS-8*	146	–10.8	–11.9	–7.2	–18.0	9	0	0	2	0
PD-L1 dimer – BMS-37*	6–100	–11.0	–12.0	–7.1	–18.1	9	0	0	1	0.97
PD-L1 dimer – BMS-105*	6–100	–10.9	–11.8	–7.8	–18.6	6	1	0	1	0.56
PD-L1 dimer – BMS-200*	80	–11.5	–12.7	–7.8	–19.3	6	2	0	1	1.17
PD-L1 dimer – BMS-202*	18	–12.1	–13.5	–7.3	–19.4	8	2	0	1	1.08
PD-L1 dimer – BMS-1001*	2–15	–12.5	–13.9	–7.2	–19.7	9	3	0	0	1.26
PD-L1 dimer – BMS-1166*	1.4	–12.9	–14.2	–6.9	–19.8	9	3	1	1	1.22

Note. $\Delta G_{Pr,trimer} = \Delta G_{Pr} + \Delta G_{AB}$; n_{HPH} – number of hydrophobic contacts; n_{HB} – number of hydrogen bonds; n_{SB} – number of salt bridges; $n_{\pi\text{-st}}$ – number of π-stacking pairs; * – complexes of PD-L1 dimer with BMS-8 (PDB code: 5j8o), BMS-37 (PDB code: 5n2d), BMS-105 (PDB codes: 6nnv, 6nmv), BMS-200 (PDB code: 5n2f), BMS-202 (PDB code: 5j89), BMS-1001 (PDB code: 6r3k), BMS-1166 (PDB code: 5niu); ** – $\Delta G_{Pr,tr}$ stands for $\Delta G_{Pr,trimer}$.

Small molecules targeting the PD-1 – PD-L1 interaction are actively sought by academic institutions and pharmaceutical companies with the hope of surpassing the success of antibodies due to expected better efficacy of small molecules as compared to antibodies because of their better tumor penetration and oral availability. Although this field is only in its initial stage, several small molecule immunomodulatory compounds at the stage of preclinical development have been reported to date [13]. Whereas atomic-level structures of their complexes with PD-L1 are known for a number of them, high-resolution structures for some of them possessing IC_{50} values in low nanomolar range are not determined to date, thus hampering the rational structure based development of efficient drugs. In the present study, based on known X-ray structures (PDB codes: 5j8o, 5j89, 5n2d, 5n2f, 5niu, 5nix, 6nm7, 6nm8), the prediction of the atomistic 3D structure of PD-L1 dimer with resveratrol was carried out. As in known X-ray structures of PD-L1 – BMS-ligand complexes, PD-L1 interacts simultaneously with two monomers of PD-L1. The analysis of the receptor – ligand complexes allowed the detection of the residues involved in dimer stabilisation. As in all previously characterised structures of the complexes of PD-L1 with BMS-SMIs, resveratrol interacts with same key interaction residues, namely with Ile54A, Tyr56A, Gln66A, Met115A, Ser117A, Ala121A, Asp122A and Ile54B, Tyr56B, Met115B, Ser117B, Ala121B, Tyr123B. Overall, the inhibition of PD-L1 immunosuppressive action occurs through multiple hydrophobic and electrostatic interactions that stabilise the trimeric complex including ligand and two monomers. Our studies show that resveratrol stabilises the $(PD\text{-}L1)_2$ – ligand trimeric complex more efficiently than known BMS-ligands and as such can be seen as the promising hit compound for drug design of therapeutics for the suppression of PD-1 – PD-L1 interaction.

Conclusion

Cancer immunomodulation involves the use of synthetic or natural agents capable of activating the immune response to impede tumor cell dissemination. The nutraceutical resveratrol, a natural polyphenolic phytoalexin that is present in red wine, red grape skin, berries, peanuts, and other natural sources, has recently been proposed as a cancer immunomodulatory molecule by either acting on immune cells or by sensitising tumor cells to the cytotoxic effects of immune cells [37]. Our computer-aided simulations combining docking with MD have shown that resveratrol locates at the center of the PD-L1 homodimer, filling a deep hydrophobic pocket that contributes multiple additional interactions between the PD-L1 monomers. Resveratrol almost perfectly duplicate the target space of BMS-SMIs, which have a common scaffold and interact with the cavity formed by two PD-L1 monomers and with key interactions with Ile54, Tyr56, Met115, Ile116, Ala121, and Tyr123, thereby blocking the PD-1 – PD-L1 interaction by inducing PD-L1 dimerisation. Due to its special structure features, very strong binding takes place between PD-L1 monomers and ligands as well as between protein monomers. This results in much higher stabilisation energy of trimeric complex of resveratrol with PD-L1 dimer as compared with the case of BMS-ligands, suggesting resveratrol as a promising hit-candidate for the design of powerful drugs for immunological therapy.

References

1. Zhang H, Chen J. Current status and future directions of cancer immunotherapy. *Journal of Cancer*. 2018;9(10):1773–1781. DOI: 10.7150/jca.24577.

2. Mellman I, Coukos G, Dranoff G. Cancer immunotherapy comes of age. *Nature.* 2014;480(7378):480–489. DOI: 10.1038/nature10673.

3. Smyth MJ. Multiple approaches to immunotherapy – the new pillar of cancer treatment. *Immunology & Cell Biology*. 2017; 95(4):323–324. DOI: 10.1038/icb.2017.9.

4. Pardoll DM. The blockade of immune checkpoints in cancer immunotherapy. *Nature Reviews Cancer.* 2012;12(4):252–264. DOI: 10.1038/nrc3239.

5. Tumeh PC, Harview CL, Yearley JH, Shintaku IP, Tayloret EJM, Robert L. PD-1 blockade induces responses by inhibiting adaptive immune resistance. *Nature.* 2014;515(7528):568–571. DOI: 10.1038/nature13954.

6. Francisco LM, Sage PT, Sharpe AH. The PD-1 pathway in tolerance and autoimmunity. *Immunological Reviews.* 2010;236(1): 219–242. DOI: 10.1111/j.1600-065X.2010.00923.x.

7. Herbst RS, Soria J-C, Kowanetz M, Fine GD, Hamid O, Gordon MS, et al. Predictive correlates of response to the anti-PD-L1 antibody MPDL3280A in cancer patients. *Nature.* 2014;515(7528):563–567. DOI: 10.1038/nature14011.

8. Mei-Miao Zhan, Xue-Qin Hu, Xiu-Xiu Liu, Ban-Feng Ruan, Jun Xu, Chenzhong Liao. From monoclonal antibodies to small molecules: the development of inhibitors targeting the PD-1/PD-L1 pathway. *Drug Discovery Today.* 2016;21(6):1027–1036. DOI: 10.1016/j.drudis.2016.04.011.

9. Zarganes-Tzitzikas T, Konstantinidou M, Gao Y, Krzemien D, Zak K, Dubin G, et al. Inhibitors of programmed cell death 1 (PD-1): a patent review (2010–2015). *Expert Opinion on Therapeutic Patents.* 2016;26(9):973–977. DOI: 10.1080/13543776.2016.1206527.

10. Zak KM, Kitel R, Przetocka S, Golik P, Guzik K, Musielak B, et al. Structure of the complex of human programmed death 1, PD-1, and its ligand, PD-L1. *Structure.* 2015;23(12):2341–2348. DOI: 10.1016/j.str.2015.09.010.

11. Verdura S, Cuyàs E, Cortada E, Brunet J, Lopez-Bonet E, Martin-Castillo B, et al. Resveratrol targets PD-L1 glycosylation and dimerization to enhance antitumor T-cell immunity. *Aging (Albany NY)*. 2020;12(1):8–34. DOI: 10.18632/aging.102646.

12. Friesner RA, Banks JL, Murphy RB, Halgren TA, Klicic JJ, Mainz DT, et al. Glide: a new approach for rapid, accurate docking and scoring. 1. Method and assessment of docking accuracy. *Journal of Medicinal Chemistry.* 2004;47(7):1739–1749. DOI: 10.1021/jm0306430.

13. Guzik K, Tomala M, Muszak D, Konieczny M, Hec A, Błaszkiewicz U, et al. Development of the inhibitors that target the PD-1/PD-L1 interaction – a brief look at progress on small molecules, peptides and macrocycles. *Molecules.* 2019;24(11):2071. DOI: 10.3390/molecules24112071.

14. Pronk S, Páll S, Schulz R, Larsson P, Bjelkmar P, Apostolov R, et al. GROMACS 4.5: a high-throughput and highly parallel open source molecular simulation toolkit. *Bioinformatics.* 2013;29(7):845–854. DOI: 10.1093/bioinformatics/btt055.

15. Huang J, MacKerell AD Jr. CHARMM36 all-atom additive protein force field: validation based on comparison to NMR data. *Journal of Computational Chemistry*. 2013;34(25):2135–2145. DOI: 10.1002/jcc.23354.

16. Jorgensen WL, Chandrasekhar J, Madura JD, Impey RW, Klein ML. Comparison of simple potential functions for simulating liquid water. *Journal of Chemical Physics.* 1983;79(2):926–935. DOI: 10.1063/1.445869.

17. Bussi G, Donadio D, Parrinello M. Canonical sampling through velocity rescaling. *Journal of Chemical Physics*. 2007;126(1):014101. DOI: 10.1063/1.2408420.

18. Parrinello M, Rahman A. Polymorphic transitions in single crystals: a new molecular dynamics method. *Journal of Applied Physics.* 1981;52(12):7182–7190. DOI: 10.1063/1.328693.

19. Darden T, York D, Pedersen L. Particle mesh Ewald: an $N \cdot \log(N)$ method for Ewald sums in large systems. *Journal of Chemical Physics.* 1993;98(12):10089–10092. DOI: 10.1063/1.464397.

20. Essmann U, Perera L, Berkowitz ML, Darden T, Lee H, Pedersen LG. A smooth particle mesh Ewald method. *Journal of Chemical Physics*. 1995;103(19):8577–8593. DOI: 10.1063/1.470117.

21. Vangone A, Schaarschmidt J, Koukos P, Geng C, Citro N, Trellet ME, et al. Large-scale prediction of binding affinity in protein-small ligand complexes: the Prodigy-Lig web server. *Bioinformatics.* 2019;35(9):1585–1587. DOI: 10.1093/bioinformatics/bty816.

22. Jiménez J, Škalič M, Martínez-Rosell G, De Fabritiis G. K_{DEEP}: protein – ligand absolute binding affinity prediction via 3D-convolutional neural networks. *Journal of Chemical Information and Modeling*. 2018;58(2):287–296. DOI: 10.1021/acs.jcim.7b00650.

23. Salentin S, Schreiber S, Haupt VJ, Adasme MF, Schroeder M. PLIP: fully automated protein – ligand interaction profiler. *Nucleic Acids Research.* 2015;43(W1):W443–W447. DOI: 10.1093/nar/gkv315.

24. Kozakov D, Hall DR, Xia B, Porter KA, Padhomy D, Yueh C, et al. The ClusPro web server for protein – protein docking. *Nature Protocols*. 2017;12(2):255–278. DOI: 10.1038/nprot.2016.169.

25. Tovchigrechko A, Vakser IA. GRAMM-X public web server for protein – protein docking. *Nucleic Acids Research.* 2006;34(supplement 2):W310–W314. DOI: 10.1093/nar/gkl206.

26. Yumeng Yan, Di Zhang, Pei Zhou, Botong Li, Sheng-You Huang. HDock: a web server for protein – protein and protein – DNA/RNA docking based on a hybrid strategy. *Nucleic Acids Research.* 2017;45(W1):W365–W373. DOI: 10.1093/nar/gkx407.

27. Lim Heo, Hasup Lee, Chaok Seok. GalaxyRefineComplex: refinement of protein – protein complex model structures driven by interface repacking. *Scientific Reports.* 2016;6(1):32153. DOI: 10.1038/srep32153.

28. Gray JJ, Moughon S, Wang C, Schueler-Furman O, Kuhlman B, Rohl CA, et al. Protein – protein docking with simultaneous optimization of rigid-body displacement and side-chain conformations. *Journal of Molecular Biology.* 2003;331(1):281–299. DOI: 10.1016/S0022-2836(03)00670-3.

29. Lyskov S, Gray JJ. The RosettaDock server for local protein – protein docking. *Nucleic Acids Research.* 2008;36(supplement 2):W233–W238. DOI: 10.1093/nar/gkn216.

30. Xue LC, Rodrigues JP, Kastritis PL, Bonvin AM, Vangone A. Prodigy: a web server for predicting the binding affinity of protein – protein complexes. *Bioinformatics*. 2016;32(23):3676–3678. DOI: 10.1093/bioinformatics/btw514.

31. Erijman A, Rosenthal E, Shifman JM. How structure defines affinity in protein – protein interactions. *PloS One.* 2014;9(10):e110085. DOI: 10.1371/journal.pone.0110085.

32. Nilofer C, Sukhwal A, Mohanapriya A, Kandueane P. Protein – protein interfaces are vdW dominant with selective H-bonds and (or) electrostatics towards broad functional specificity. *Bioinformation.* 2017;13(6):164–173. DOI: 10.6026/97320630013164.

33. Bender BJ, Cisneros A III, Duran AM, Finn JA, Fu D, Lokits AD, et al. Protocols for molecular modeling with Rosetta3 and RosettaScripts. *Biochemistry.* 2016;55(34):4748–4763. DOI: 10.1021/acs.biochem.6b00444.

34. Sukhwal A, Sowdhamini R. PPCheck: a webserver for the quantitative analysis of protein – protein interfaces and prediction of residue hotspots. *Bioinformatics and Biology Insights.* 2015;9:141–151. DOI: 10.4137/BBI.S25928.

35. Morris GM, Huey R, Olson AJ. Using AutoDock for ligand-receptor docking. *Current Protocols in Bioinformatics*. 2008;24(1):8.14.1–8.14.40. DOI: 10.1002/0471250953.bi0814s24.

36. Andrei SA, Sijbesma E, Hann M, Davis J, O'Mahony G, Perry MWD, et al. Stabilization of protein – protein interactions in drug discovery. *Expert Opinion on Drug Discovery*. 2017;12(9):925–940. DOI: 10.1080/17460441.2017.1346608.

37. Trung LQ, An DTT. Is resveratrol a cancer immunomodulatory molecule? *Frontiers in Pharmacology.* 2018;9:1255. DOI: 10.3389/fphar.2018.01255.

Received by editorial board 30.06.2020.